6.7 FIELD-CAMPAIGN RADAR DATA COLLECTED IN THE CONTEXT OF THE TRMM CLIMATOLOGY: COMPARISONS OF OBSERVED STORM MORPHOLOGY AND VALIDATION OPPORTUNITIES

Stephen W. Nesbitt*, Robert Cifelli, and Steven A. Rutledge
Colorado State Univerisity, Fort Collins, Colorado

Edward J. Zipser
University of Utah, Salt Lake City, Utah

1. INTRODUCTION

Many field campaigns using ground-based radars have been undertaken over the past four decades in the Tropics, and the data collected have been instrumental in improving our physical understanding of the global climate system. Unfortunately, the timescale of the radar observations collected in field campaigns (on the order of a month to several months) is less than the period of many modes of Tropical atmospheric variability that occur on longer timescales. Examples include seasonal variability, ENSO and the MJO, which most certainly influence the types, microphysics, and kinematics of rainfall systems in a given region, such that any climatology of the properties of rainfall systems derived from field campaign data may not be completely representative of the "true climatology" of rainfall systems in a given region.

Routine radar observations are not widely available in the Tropics, so, until recently, one had to rely solely on field campaign data as our "ground truth" of the rainfall regimes present in the Tropics. With the launch of the Tropical Rainfall Measuring Mission (TRMM) satellite in December 1997, the precipitation radar (PR) has allowed the retrieval of snapshots of vertical reflectivity profiles it overflies. Thus, TRMM provides the opportunity to examine the climatology of rainfall systems on timescales longer than those seen by individual field campaigns. However, since TRMM only samples relatively infrequent snapshots of the radar reflectivity field in a given region, the ground-based radar remains the tool of choice for examining many characteristics of precipitating systems, including their life cycle and the local variability in rainfall in a given area, for example.

The desire to intercompare radar data among field campaigns provides the motivation to use the satellite to understand the context of field-campaign-observed rainfall systems in the perspective of the satellite climatology, particularly in their rainfall and convective intensity and morphology characteristics, and where those storms fit into the statistical distribution of storms using such characteristics. The PR's calibration is stable and accurate to within 1 dBZ (Iguchi et al. 2000), and Heymsfield et al. (2000) has shown that the PR is, in large part, a reliable standard to compare ground-based radar data with when the PR's relatively low sensitivity and resolution are taken into account.

* *Corresponding author address:* Stephen W. Nesbitt, Dept. of Atmospheric Science, Colorado State University, Fort Collins, CO 80523-1371;
E-mail: snesbitt@radarmet.atmos.colostate.edu

2. TRMM CLIMATOLOGY: THE PF DATABASE

The TRMM PR and TMI observations have been collocated to identify a database of individual precipitation features (PFs, see Nesbitt et al. 2000 for complete details) within the PR 220 km-wide PR swath for the periods Dec. 1997-Nov. 2000 and Dec. 2001-Nov. 2002. The intervening period was not processed due to TRMM's altitude boost which caused PR data problems during Aug.-Nov. 2001 and the TRMM boost subsequently reduced the horizontal resolution of the instruments by 15%. PFs are defined as contiguous areas ≥ 4 PR pixels in area (a PR pixel was 4.3 km^2 in area before the TRMM boost) with PR near surface reflectivity ≥ 20 dBZ (above the PR's minimum detectable signal ~ 17 dBZ) or 85 GHz polarization corrected temperature (PCT) ≤ 250 K. Note that the former condition solely identifies a large majority of PF pixels. Once a feature has been identified, several characteristics related to its horizontal and vertical properties are recorded, for example its location, time of occurrence, total rain volume, convective-stratiform partitioning (according to the TRMM 2A23 product), echo top heights, and about 25 other characteristics of each PF. These observations from individual overpasses of the satellite can be composited to form a climatology of PFs within a given region, given sufficient integration time (for example, 23 days is required to observe the entire diurnal cycle). When comparing the satellite climatology with the ground based dataset, the Tropics-wide PF database is subsetted in a grid box surrounding the location of the ground based radar.

3. PFS DURING THE EPIC FIELD CAMPAIGN

The NOAA R/V Ronald H. Brown (RHB) C-band radar was stationed within the East Pacific warm-pool/ITCZ at roughly 10°N, 95°W (see Fig. 1) during the period September 12-October 1, 2001 for the East Pacific Investigation of Climate Processes in the Coupled Ocean-Atmosphere System (EPIC, Raymond et al. 2003) field experiment. During this period, it collected volume scans of radar reflectivity out to r=150 km at 10 minute intervals. According to Petersen et al. (2003), calibration with TRMM and a nearby S-band vertical profiler yielded no detectable calibration offset in EPIC RHB reflectivity, so no correction was applied. Clutter and second trip were removed using the NASA TRMM Office QC algorithm. The polar data were corrected for attenuation at C-band using a relationship following Patterson et al. (1979). The data were then gridded using NCAR REORDER to a resolution of 4.3 × 4.3 km in the horizontal and 0.5 km in the vertical using the Cressman

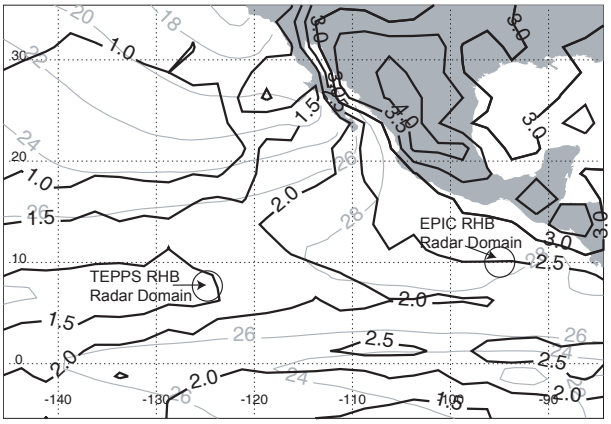

Fig. 1. Map of: TRMM ASO 1998-2000 PR mean maximum height of the 30 dBZ echo in PFs (km, black lines), NCEP ASO 1981-97 SST climatology (°C, gray lines), and on-station locations of EPIC and TEPPS radars.

weighting scheme with a radius of influence of 4.3 km in the horizontal and 1 km in the vertical (set to be larger in than the vertical grid spacing to avoid data gaps at far ranges) corresponding as closely as possible with the TRMM PR horizontal resolution, with half the vertical resolution. Rain rates within the EPIC dataset were calculated from

$$Z = 218\ R^{1.6},$$

a relationship derived from 2D-P data collected aboard the NCAR C-130 aircraft during the experiment (note this relationship differs from the total path attenuation-adjusted relation used in TRMM, see Iguchi et al. 2000).

The EPIC RHB data were then processed to locate PFs as in TRMM PF processing, with contiguous areas greater than 4 pixels with 2 km reflectivity ≥ 20 dBZ recorded as PFs in the EPIC data set (note that no 85 GHz threshold was applied, as no observations were available). Radar reflectivity structure statistics are compiled as in the TRMM dataset (areas, maximum echo top heights, etc.). Convective-stratiform partitioning was applied to the ground based data using the methodology of Steiner et al. (1995); note that this methodology uses horizontal reflectivity gradients to identify convection, while the TRMM 2A23 algorithm uses both horizontal and vertical gradients of reflectivity (the latter is used to identify a bright band in stratiform regions). These differences in methodology likely cause a partitioning bias, however the TRMM technique cannot be applied to ground based data due to poor vertical resolution (and smearing of the bright band). Future work will seek to quantitatively examine the implications of this difference.

Upon combining the entire EPIC field campaign, 25,300 PFs were found in the EPIC radar dataset, compared with 2,490 TRMM PFs during ASO 1998-2000 over a 5° box centered over the EPIC domain.

4. CONTEXT OF THE EPIC FIELD CAMPAIGN

The EPIC domain was located along a climatological north-south gradient in SST, with warmer temperatures to the north (Fig 1). The area is also within 500 km of land to the northeast. Both of these factors likely lead to the north-south gradient in TRMM-observed convective intensity as indicated by the mean PF maximum height of the 30 dBZ echo. Intraseasonally, the vertical and horizontal structures of precipitation features in the area during this season are also strongly modulated by the passage of Tropical easterly waves (Petersen at al. 2003). Unfortunately, the TRMM boost and sampling constraints do not allow one to one comparisons of the time series of PR and ground based radar reflectivity statistics in 2001, so this study compares seasonal distributions from other available years.

The cumulative distribution functions (CDFs) of radar reflectivity vertical profiles separated into convective and stratiform profiles from the EPIC RHB radar and the TRMM PR appear in Fig. 2. The distributions appear very similar between the two radars for convective points above the minimum detectable signal of the PR (~17 dBZ), especially below 10 km. Above 10 km, the PR is considerably weaker than the RHB radar, likely due to the lack of sensitivity in weak reflectivity regions aloft. Note that the 99.99th percentile of reflectivity values sampled by TRMM are significantly stronger (by

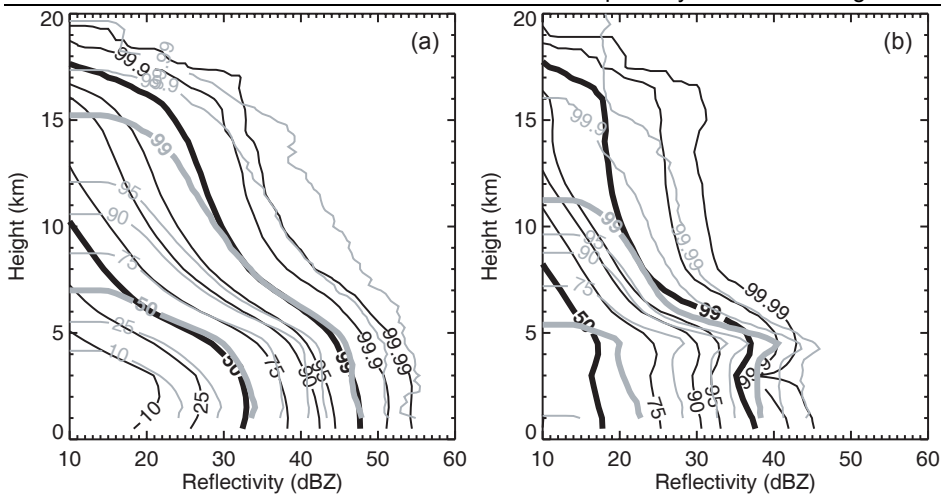

Fig. 2. EPIC RHB 2001 (dark lines) and TRMM PR SON 2002 (grey lines) height-reflectivity CDFs for (a) convective and (b) stratiform points.

several dBZ) than those sampled during EPIC, especially in the mixed phase region.

In stratiform regions (b), the higher vertical resolution of the PR allows it to resolve the bright band more distinctly, and below the freezing level, the PR has more intense reflectivity distributions. Above the freezing level, the PR's reflectivity distributions are significantly weaker than the RHB's, the lack of sensitivity is likely a large factor here in the low reflectivity snow regions aloft in stratiform pixels.

5. COMPARISONS OF CDFS OF PF PARAMETERS

Comparisons of the statistics of individual storm parameters from the PF database are presented in this section. Specifically, the statistics derived from 3 ASO seasons from the TRMM database (1997-2000) in a 5° × 5° box centered on the EPIC RHB radar are compared with statistics from the 3-week long RHB dataset. (Note: the selection of a 5° box for subsetting of the TRMM data is arbitrary, comparisons using a 2.5° box - roughly the area sampled by the ground radar - were very similar but yielded about ¼ the sample size).

CDFs of maximum echo top height (Fig. 3a) indicate for all reflectivity thresholds, the EPIC radar has higher maximum echo top heights. This is especially true for the higher reflectivity thresholds (i.e. 30 and 40 dBZ). This finding is in contrast to the similar reflectivity CDFs for all profiles shown in Fig 2. The exact cause of this remains a topic for future study, but several hypotheses for this difference include: 1) sampling of a number of intense storms in EPIC that skewed the echo top height distrubutions towards being more intense, 2) the difference in reflectivity weighting caused by the Cressman scheme in ground-based EPIC data that may weight higher reflectivity cores more than the beam averaging of the PR, 3) The lack of sensitivity of the PR may bias its echo top height distributions low. The results of Heymsfield et al. (2000) and Durden et al. (2003) also that maximum reflectivities tend to be reduced when compared with ground and airborne radars, hypothesized to be due to non-uniform beam filling effects in convective cores.

PF area distributions (Fig. 3b) are very similar between EPIC and TRMM, despite the differing sample volumes of the two instruments. Specifically, the fact that the two radars have similar sampling in the cross-track direction of the PR (~220-300 km), but PR has an "unlimited" sample volume in the along-track direction (compared to finite sampling of the ground-based radar). The slight positive bias in area towards TRMM PFs may be due to this, in addition to the fact that 85 GHz pixels with PCT ≤ 250 K are included in the TRMM area (this is a small fraction of the pixels viewed).

Convective-stratiform distributions are similar in shape (Fig. 3c), but their magnitudes are quite different between EPIC and TRMM. This is not surprising given the different schemes used for convective stratiform portioning in the two datasets. It appears that TRMM is much less likely to assign rainfall as convective compared with the Steiner et al. (1998) algorithm (34% of TRMM PFs have no convection, compared with only 8% of EPIC PFs). The median (50^{th} percentile) area of rainfall convective within each feature is about 13% from TRMM, while it is about 42% from EPIC. The fraction of rainfall convective also differs by a large amount between the two datasets; from TRMM the mean fraction of rain convective is about 42%, while from TRMM it is about 73%. The rather high fraction of rainfall convective found in EPIC is similar to the value of 85% found by Petersen et al. (2003), who used EPIC radar data gridded at higher resolution (2km) and a slightly different partitioning algorithm (Steiner and Houze 1993). This difference in convective-stratiform rain volume may be due to differences in the storms observed or the differing Z-R relationships used, but also may be due to differences caused by the methodology differences of the rainfall partioning. This uncertainty needs to be adderssed since it has important implications on retrievals of the vertical profile of latent heating that use partioning information to describe the shape of the prescribed heating profile (e.g. Tao et al. 1993).

6. COMPARISONS OF PARTIONED NEAR SURFACE REFLECTIVITIES AND RAIN RATES

PDFs of "near surface" reflectivities from TRMM during ASO 2002 are compared with EPIC 2 km values in Fig. 4a (no PF definition is applied here, thus the inclusion of values < 20 dBZ). Most striking is the influence of the minimum detectable signal of the PR in the stratiform reflectivity distribution. This cuts out the lower half of the stratiform reflectivity distribution from the PR distribution. The convective distribution from the PR is also not as broad as those seen in EPIC, the location of the modal value of the distribution is 3 or so dBZ lower in reflectivity space from the PR. The tail of the PR distribution at the high reflectivity end is also quite a bit shorter than from EPIC (this may be a reflection of the lower echo top height distributions shown in Fig. 3).

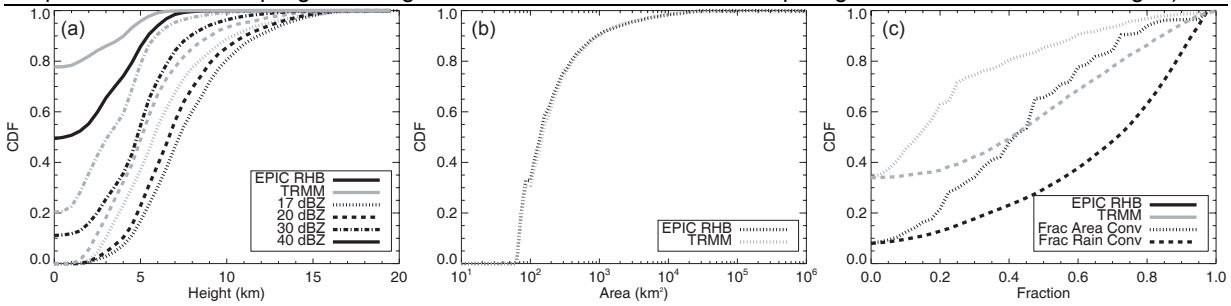

Fig. 3. EPIC RHB 2001 (dark lines) and TRMM PR SON 1998-2000 (grey lines) (a) CDFs of 17, 20, 30, and 40 dBZ PF maximum echo top height, (b) PF area, and (c) fraction of area and rain classified as convective.

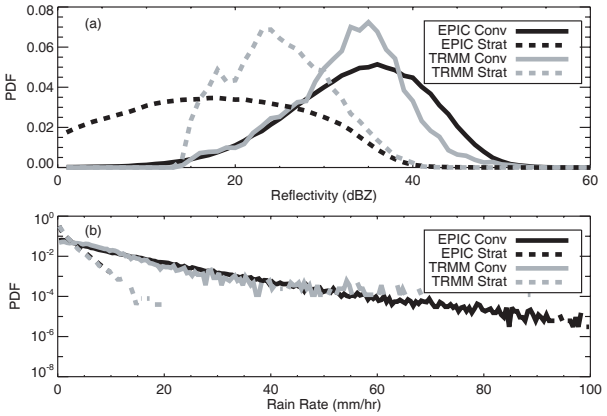

Fig. 4. EPIC (dark lines) and TRMM (grey lines) PDFs of convective (solid) and stratiform (dashed) "near surface" (a) radar reflectivity and (b) rain rates.

Rain rate distributions between the two datasets appear more similar (Fig. 4b) than reflectivity distributions, although TRMM reports more stratiform rain rates to nearly 20 mm hr^{-1}, which are rain rates higher than usually thought to be stratiform (the Steiner et al. 1998 algorithm actually sets all reflectivities > 40 dBZ–corresponding to rain rates of about 10 mm hr^{-1}–as convection). Convective rain rate distributions have somewhat similar slope between TRMM and EPIC, however, TRMM has a lower (higher) relative frequency of points between 15 and 45 (55 and 70) mm hr^{-1}, and a distinct lack of points above 70 mm hr^{-1}. The latter fact may reflect a sampling bias in the relatively smaller TRMM dataset or smearing of the convective cores by the PR. The similarity is remarkable, however, considering the (presumed) differences in the local (EPIC) vs. global (TRMM) Z-R relationships used.

7. SUMMARY AND FUTURE WORK

This paper outlines the methodology and preliminary results in an effort to compare radar datasets comparing ground based radar datasets from field campaigns with the satellite-derived climatology derived from the TRMM satellite. It was found that the sizes and total radar reflectivity distributions with height in precipitation features were quite similar when derived from the EPIC and the TRMM climatology in the surrounding area and season. However, several derived parameters, including echo top heights, convective-stratiform portioning, and rain rate distributions were quite different. These differences were attributed to differences in the systems observed (sampling of differing convective regimes, for example), differing spatial interpolation schemes (interpolation of the ground based radar data to the PR's sampling), differing convective-stratiform separation schemes (which produced highly differing convective rain fraction), and differing rain relations used in the study. Because of the differences in the instruments, it is impossible to exactly match retrieval schemes; however future work will aim to reduce biases from the differing methods (i.e. testing different interpolation schemes in the ground-based radar data).

This study is in its infancy; the eventual goal of this work will be to use ground based radar data from several field campaigns to address many of the TRMM validation issues outlined herein, as well as using the TRMM satellite to place the field campaign radar datasets in their proper climatological context. Field experiments that will be analyzed include the Maritime Continent Thunderstorm Experiment (MCTEX), the Tropical Eastern Pacific Process Study (TEPPS), the TRMM-Large Biosphere Atmosphere (LBA) experiment, The Kwajalein Experiment (KWAJEX).

Acknowledgements. The authors wish to thank all those involved in the TRMM mission as well as those who worked hard to collect data in the field. Thanks to Baike Xi for her TRMM data processing assistance, David Wolff for EPIC radar QC, M. Anagnostou and C. Morales for TRMM-EPIC radar calibration, and Walt Petersen for preliminary EPIC results and discussion. This work was funded under EPIC NSF Grant ATM-0002256 and NASA TRMM grant NAG5-9642 (Ramesh Kakar).

8. REFERENCES

Durden, S. L., E. Im, Z. S. Haddad, and L. Li, 2003: Comparison of TRMM precipitation radar and airborne radar data. *J. Appl. Meteor.*, **42**, 769-774.

Heymsfield, G. M., B. Geerts, and L. Tian, 2000: TRMM precipitation radar reflectivity as compared with high-resolution airborne and ground-based radar measurements. *J. Appl. Meteor.*, **39**, 2080-2102.

Iguchi, T., T. Kozu, R. Meneghini, J. Awaka, K. Okamoto, 2000: Rain-profiling algorithm for the TRMM precipitation radar. *J. Appl. Meteor.*, **39**, 2038-2052.

Nesbitt, S. W., E. J. Zipser, and D. J. Cecil, 2000: A census of precipitation features in the Tropics using TRMM: Radar, passive microwave, and lightning observations. *J. Climate*, **13**, 4087-4106.

Patterson, V. L., M. D. Hudlow, P. J. Pytlowany, F. P. Richards, and J. D. Hoff, 1979: GATE radar rainfall processing system. NOAA Tech. Memo. EDIS 26, NOAA, Washington, DC, 34 pp.

Petersen, W. A., R. Cifelli, D. J. Boccippio, S. A. Rutledge and C. Fairall, 2003: Convection and easterly wave structure observed in the East Pacific warm-pool during EPIC 2001. *J. Atmos. Sci.*, in press.

Raymond, D. J., Raga, G., C. Bretherton, J. Molinari, C. Lopez-Carrillo, and Z. Fuchs, 2003: Dynamics of the Intertropical Convergence Zone of the East Pacific. *J. Atmos. Sci*., in press.

Steiner, M., and R. A. Houze, Jr., 1993: Three-dimensional calidation at TRMM ground truth sites: Some early results from Darwin, Australia. Preprints, *26th Conf. on Radar Meteorology,* Norman, OK, Amer. Meteor. Soc., 417-420.

Steiner, M., R. A. Houze, Jr., and S. E. Yuter, 1995: Climatological characterization of three-dimensional storm structure from operational radar and rain gauge data. *J. Appl. Meteor.*, **34**, 1978-2007.

Tao, W.-K., S. Lang, J. Simpson, and R. Adler, 1993: Retrieval algorithms for estimating the vertical profiles of latent heat release: Their applications for TRMM. *J. Meteor. Soc. Japan*, **71**, 685-700.